magnetochemistry

MDPI

Article

Torque-Detected Electron Spin Resonance as a Tool to Investigate Magnetic Anisotropy in Molecular Nanomagnets

María Dörfel [1], Michal Kern [1], Heiko Bamberger [1], Petr Neugebauer [1], Katharina Bader [1], Raphael Marx [1], Andrea Cornia [2], Tamoghna Mitra [3], Achim Müller [3], Martin Dressel [4], Lapo Bogani [4,†] and Joris van Slageren [1,*]

1 Institut für Physikalische Chemie, Universität Stuttgart, Pfaffenwaldring 55, 70569 Stuttgart, Germany; mariadorfel@gmail.com (M.D.); m.kern@ipc.uni-stuttgart.de (M.K.); heiko.bamberger@ipc.uni-stuttgart.de (H.B.); petr.neugebauer@ipc.uni-stuttgart.de (P.N.); katharina.bader@ipc.uni-stuttgart.de (K.B.); r.marx@ipc.uni-stuttgart.de (R.M.)

2 Department of Chemical and Geological Sciences & INSTM Research Unit, University of Modena and Reggio Emilia, via G. Campi 103, I-41125 Modena, Italy; andrea.cornia@unimore.it

3 Fakultät für Chemie, Universität Bielefeld, 33501 Bielefeld, Germany; tamoghnamitra@yahoo.co.in (T.M.); a.mueller@uni-bielefeld.de (A.M.)

4 Physikalisches Institut, Universität Stuttgart, Pfaffenwaldring 57, 70569 Stuttgart, Germany; dressel@pi1.physik.uni-stuttgart.de (M.D.); lapo.bogani@materials.ox.ac.uk (L.B.)

* Correspondence: slageren@ipc.uni-stuttgart.de; Tel.: +49-711-6856-4380

† Present address: Department of Materials, University of Oxford, 16 Parks Road, Oxford OX1 3PH, UK.

Academic Editors: Marius Andruh and Liviu F. Chibotaru

Received: 4 March 2016; Accepted: 26 April 2016; Published: 6 May 2016

Abstract: The method of choice for in-depth investigation of the magnetic anisotropy in molecular nanomagnets is high-frequency electron spin resonance (HFESR) spectroscopy. It has the benefits of high resolution and facile access to large energy splittings. However, the sensitivity is limited to about 10^7 spins for a reasonable data acquisition time. In contrast, methods based on the measurement of the deflection of a cantilever were shown to enable single spin magnetic resonance sensitivity. In the area of molecular nanomagnets, the technique of torque detected electron spin resonance (TDESR) has been used sporadically. Here, we explore the applicability of that technique by investigating molecular nanomagnets with different types of magnetic anisotropy. We also assess different methods for the detection of the magnetic torque. We find that all types of samples are amenable to these studies, but that sensitivities do not yet rival those of HFESR.

Keywords: magnetic resonance; molecular nanomagnet; magnetic anisotropy

1. Introduction

Molecular nanomagnets (MNMs) are mono- or polynuclear complexes of p-, d- and/or f-block elements [1]. MNMs can possess a range of interesting properties, including slow relaxation of the magnetic moment, quantum tunneling, magnetocaloric effects, and quantum coherence [2–5]. The first of these properties originates from magnetic anisotropy, which causes the magnetic response of the system to depend on the orientation of an applied magnetic field in the molecular coordinate frame. Under favorable circumstances, such an orientation dependence can engender an energy barrier between the up- and down-orientations of the magnetic moment. Magnetic anisotropy manifests itself in a range of magnetic interactions, including the Zeeman interaction (g-value anisotropy), the exchange interaction (anisotropic and antisymmetric exchange), zero-field splitting (in ions without first-order orbital angular momentum) and crystal field splitting (in f-elements).

Magnetic anisotropy can be investigated by several experimental techniques, such as magnetometry [6,7], far-infrared spectroscopy [8,9], neutron scattering [10,11], and specific heat measurements [12]. However, probably the most popular method is that of high-frequency electron spin resonance (HFESR) spectroscopy. It delivers high g-value-resolution, especially important for biological systems [13]. Importantly for the subject of this article, it allows experimental access to large energy splittings, such as those associated with magnetic anisotropy in MNMs [14]. It has also been used for the determination of anisotropic exchange interactions [15]. Finally, it can be operated in field and frequency domains [16]. However, the ultimate sensitivity of HFESR techniques, where the transmission or reflection of microwave photons is detected, is likely to be worse than a million spins. Indeed, the direct detection of microwave photons is an intrinsically low-sensitivity method, as microwave photons carry very small energies compared to, for instance, photons in the visible range. With the drive of the field to investigate (sub)monolayers of MNMs for applications in spintronic devices [17,18] this sensitivity is not sufficient. Alternative electron spin resonance (ESR) detection methods include those where the change in magnetization due to magnetic resonance is measured by superconducting interference device (SQUID) or Hall bar sensors [19]. Some of us as well as others have developed the technique of torque-detected electron spin resonance (TDESR) spectroscopy for the investigation of molecular nanomagnets [20–22]. This technique relies on the effect of magnetic resonance on magnetic torque $\boldsymbol{\tau} = \mathbf{M} \times \mathbf{B}$ and hence on the deflection of a cantilever on which the sample is mounted. This deflection is measured by recording the change in capacitance between the cantilever arm and a parallel plate (cantilever torque magnetometry, CTM). In other systems, cantilever-detected electron spin resonance was shown to reach single spin sensitivity [23]. For this method to work, the presence of magnetic anisotropy is essential to ensure noncollinearity of the magnetization $\mathbf{M}$ and the magnetic field $\mathbf{B}$ [24]. The frequency resolution is given by the monochromaticity of the source, which is in the 10^1 MHz range. The field resolution depends on the field homogeneity, which is 0.1% over one cm radius, corresponding to 10 G in a 1 T field. However, typical samples used here are of mm size, and, in practice, the field resolution is better than 1 G. Thus far, our investigations were limited to a single sample with a large zero-field splitting, namely $[Fe_4(L)_2(dpm)_6]$ (Fe_4) where Hdpm is 2,2,6,6-tetramethyl-3,5-heptanedione (also known as dipivaloylmethane) and H_3L is (*R*,*S*)-2-hydroxymethyl-2-(2-methyl-butoxymethyl)propane-1,3-diol [20,21]. It is now essential to establish the ability of the technique to probe other sources of magnetic anisotropy, as well as to explore alternative detection methods.

Here, we present new TDESR results, where we exploit optical rather than capacitive detection of cantilever deflection. In addition, we expand the range of investigated samples to include $[Mn_{12}O_{12}(OAc)_{16}(H_2O)_4]\cdot 2AcOH\cdot 4H_2O$ ($Mn_{12}Ac$), $K_6[V_{15}As_6O_{42}(H_2O)]\cdot 8H_2O$ (V_{15}) and $(PPh_4\text{-}d_{20})_2[Cu(mnt)_2]$ (Cu-mnt), where H_2mnt is maleonitriledithiol. In these samples, the magnetic anisotropy originates from zero-field splitting, antisymmetric exchange interactions and g-value anisotropy, respectively.

2. Results

Previous TDESR measurements [20,21,25] relied on capacitive detection of cantilever deflection due to magnetic torque (capacitively-detected (CD-)TDESR). To this end the capacitance between the CuBe cantilever (on which the sample is mounted) and a copper bottom plate is measured (Figure 1a). The cantilever is mounted on a movable sample holder, allowing for sliding between the aperture position, for alignment of the microwave source (100–1000 GHz), and the cantilever position for measurement. This setup was rather sensitive to electronic noise. Measurement of cantilever deflection is also at the heart of atomic force microscopy methods, in which case the deflection is detected by means of a laser beam reflected by the cantilever. Given that force microscopy methods enable measurement of single spins [23], we have considered an alternative measurement setup [26]. In this novel setup, the back plate of the cantilever sample holder is removed and the light spot of

a laser external to the optical cryomagnet is focused on the back of the cantilever. The shift in the reflected laser spot, determined by a position-sensitive detector (PSD), is a direct measure of cantilever deflection (optically-detected (OD-)TDESR), Figure 1b). Figure 1c (top panel) shows the measured shift as a function of the applied field under microwave irradiation at a constant frequency of 190 GHz (field-sweep TDESR), recorded on a single crystal of Fe_4. The broad background is due to the field dependence of the magnetic torque, which is typical for systems with large zero-field splittings [27]. The sharp peaks are due to magnetic resonance transitions within the $S = 5$ ground spin multiplet of the molecule. By fitting the broad background with a spline, the magnetic resonance lines can be seen more clearly (Figure 1c, bottom panel). As for traditional ESR, the line intensities in TDESR are relative, not absolute. The TDESR line intensity is a function of sample amount, of radiation intensity, of the size of the radiation focus, of the spin-lattice relaxation rate and of the thermal coupling to the heat bath [28]. Quantitative simulation of the line intensities would require in-depth investigation of these factors, a task well beyond the scope of the present study. These results show a similar signal-to-noise ratio compared with previous data obtained by capacitive detection [25]. Considering the size of the samples and the achieved signal-to-noise ratios, we estimate that the minimum number of spins that can be detected on the order of 10^{12}. Sensitivity is thus several orders of magnitude worse than in the case of HFESR.

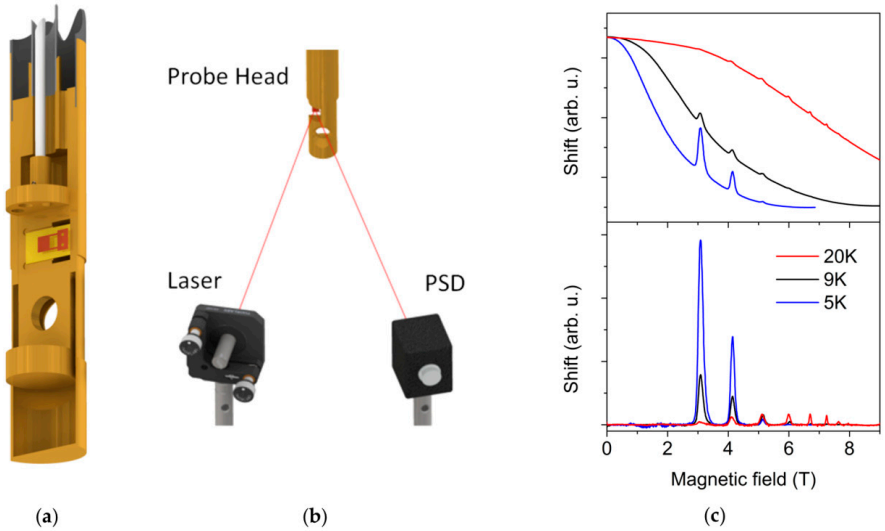

Figure 1. (**a**) schematic drawing of the bottom part of the sample rod, showing the sliding sample holder. This allows switching between an aperture for alignment purposes, and the cantilever (dark brown, with yellow bottom plate); (**b**) setup for optical detection of the cantilever deflection by means of a laser and position-sensitive detector (PSD); (**c**) field-domain torque-detected electron spin resonance (TDESR) measurements on a single crystal of Fe_4 with the crystal *c*-axis at 32° from the easy axis and different temperatures as indicated, with raw curves on top and the baseline-corrected spectra on the bottom.

As a further test, we have focused on the archetypal single-molecule magnet $Mn_{12}Ac$, which has an $S = 10$ ground spin state. The magnetic properties in the ground state can be described well by means of the spin Hamiltonian:

$$\mathcal{H} = \mu_B \mathbf{B} \cdot \mathbf{g} \cdot \hat{\mathbf{S}} + D\left(\hat{S}_z^2 - \frac{1}{3}S(S+1)\right) + E\left(\hat{S}_x^2 - \hat{S}_y^2\right) + \sum_{q=0}^{4} B_4^q \hat{O}_4^q, \quad (1)$$

where **B** is the magnetic field vector, **g** is the g matrix, D and E are the second-rank axial and rhombic zero-field splitting parameters, respectively, and B_4^q are the fourth-rank zero-field splitting parameters.

The 2.5 × 0.5 × 0.5 mm^3 crystal was oriented with its easy axis in the rotation plane (Figure S1) and both CD (Figure 2a) and OD (Figure 2b) frequency-domain TDESR spectra were recorded at 7 K. CD-CTM measurements served to determine the exact orientation of the easy axis, exploiting the fact that the torque signal vanishes when the easy axis and the magnetic field are parallel. Note that in frequency-domain spectra, the field is kept constant and the torque signal without irradiation is thus also constant at each probed field value. The two sets of spectra display peaks in the region around 300 GHz and in the region around 250–260 GHz. These peaks, whose positions depend on the external field strength, are attributed to magnetic resonance transitions from $|M_S = \pm 10\rangle$ to $|\pm 9\rangle$ and from $|\pm 9\rangle$ to $|\pm 8\rangle$, respectively. The peaks in frequency-domain spectra have a much more ragged look than those in field-domain spectra, due to variations of the source intensity as a function of frequency and due to standing waves in the radiation beam. The CD-TDESR spectra could be reproduced well by using published [29] spin Hamiltonian parameters $g_{||} = 1.93$, $g_{\perp} = 1.96$, $D = -0.46$ cm^{-1}, $B_4 = -2.2 \times 10^{-5}$ cm^{-1}, $|B_4{}^4| = 4 \times 10^{-5}$ cm^{-1}. The optically detected (OD-)TDESR spectra show essentially the same features, with differences in peak positions due to the different angle between the *c*-axis and the magnetic field. The quality of the CD- and OD-TDESR spectra is very similar. OD-TDESR has the disadvantage that the rotation angle of the cantilever is limited by the aperture of the optical windows, and angle-dependent measurements are thus severely hampered. Therefore, in the following, we have focused on capacitively detected measurements only.

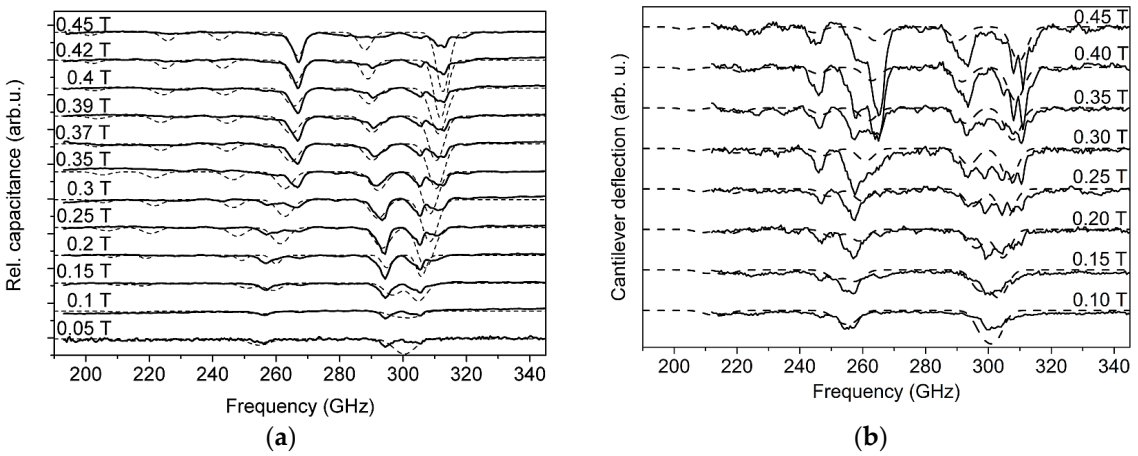

Figure 2. (**a**) capacitively detected frequency-domain TDESR spectra recorded on a single crystal of Mn_{12}Ac with the applied field 4° from the easy axis (*c*), at 7 K and different fields as indicated; (**b**) optically detected frequency-domain TDESR spectra recorded on a single crystal of Mn_{12}Ac with the crystal *c*-axis 45° from the field, at 7 K and different fields as indicated. In both panels, solid lines are experimental data and dashed lines represent the simulations.

The origin of magnetic anisotropy in Mn_{12}Ac is the same as in Fe_4, *i.e.*, zero-field splitting of the ground spin state. To explore if other sources of anisotropy also suffice and allow for successful TDESR studies, we next focused on V_{15}, which consists of fifteen $S = ½$ VO^{2+} ions [30]. Magnetically, this compound has a layered structure consisting of two strongly antiferromagnetically coupled vanadyl hexagons (Figure S2). At the temperatures relevant to this studies, these hexagons can be considered diamagnetic. The two hexagons sandwich three further vanadyl ions, which are more weakly antiferromagnetically exchange coupled. In antiferromagnetically coupled equilateral $S = ½$ triangles, the ground manifold comprises two degenerate states with $S = ½$. In practice, a small energy gap is found between these two states. There has been a long debate on whether this splitting is due to the occurrence of antisymmetric exchange interactions or to an isosceles distortion of the

triangle [31–34]. A suitable spin Hamiltonian for the description of the low temperature properties of V_{15} is:

$$\mathcal{H} = \mu_B \mathbf{B} \cdot \mathbf{g} \cdot \hat{\mathbf{S}} + J' \hat{\mathbf{S}}_1 \cdot \hat{\mathbf{S}}_2 + J \left(\hat{\mathbf{S}}_2 \cdot \hat{\mathbf{S}}_3 + \hat{\mathbf{S}}_1 \cdot \hat{\mathbf{S}}_3 \right) + \mathbf{G} \cdot \left(\hat{\mathbf{S}}_1 \times \hat{\mathbf{S}}_2 + \hat{\mathbf{S}}_2 \times \hat{\mathbf{S}}_3 + \hat{\mathbf{S}}_1 \times \hat{\mathbf{S}}_3 \right), \quad (2)$$

where J' and J are the isotropic exchange coupling constants ($J' = J$ for an equilateral triangle) and $\mathbf{G}$ is the antisymmetric exchange interaction vector.

We have performed CTM measurements on a $1.0 \times 0.5 \times 0.5$ mm^3 single crystal of V_{15} (Figure 3a). The torque signal is much weaker for V_{15} compared to Mn_{12} for similar crystal sizes. For a satisfactory reproduction of CTM curves with a minimal model, it turns out that inclusion of the parameters $g_{||} = 1.95$, $g_{\perp} = 1.98$, $J' = J = 0.847$ cm^{-1} and $\mathbf{G} = (0, 0, 0)$ suffices [35]. Hence, g value anisotropy is sufficient to observe a nonzero magnetic torque signal and CTM does not help distinguishing between the two aforementioned scenarios. It must be noted here that the cantilever torquemeter is not calibrated and a quantitative measurement of the magnetic torque is therefore not possible. Frequency domain CD-TDESR spectra (Figure 3b) display a single clear resonance line for each applied magnetic field. This resonance line is attributed to the $|S = 3/2, M_S = -3/2\rangle$ to $|3/2\ -1/2\rangle$ transition with possible contributions from the $|3/2 - 1/2\rangle$ to $|3/2 + 1/2\rangle$, $|3/2 + 1/2\rangle$ to $|3/2 + 3/2\rangle$, and $|1/2 - 1/2\rangle$ to $|1/2 + 1/2\rangle$ transitions (Figure S2). The resonance line positions can be very well accounted for by spin Hamiltonian in Equation (2) with the same parameters used to reproduce CTM curves. This demonstrates that anisotropy due to antisymmetric exchange interactions and/or g-value anisotropy is enough for the successful measurement of TDESR spectra.

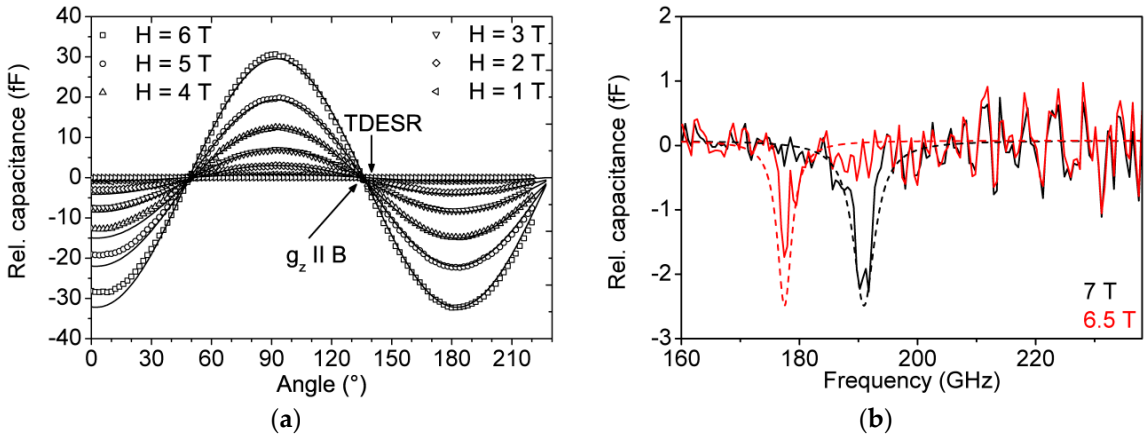

Figure 3. (**a**) capacitance as a function of angle for a single crystal of V_{15} at 7 K and different fields as indicated. Symbols represent experimental data while solid lines are calculated data; (**b**) frequency-domain CD-TDESR spectra recorded on a single crystal of V_{15} with the field 2° from the unique crystal [1 1 1]-axis, at 2 K and different fields as indicated. The solid and dashed lines are the measured and simulated spectra, respectively.

In order to definitively clarify whether g-value anisotropy alone allows successful measurement of TDESR spectra, we have expanded our investigation to the mononuclear copper(II) complex Cu-mnt. Here, the only possible source of magnetic anisotropy is the g-value anisotropy of the $S = ½$ copper(II) ion. Some of us have recently reported on the quantum coherent properties of this molecule [36]. A complication is that the compound crystallizes in a monoclinic space group, leading to two differently oriented molecules in the unit cell (Figure S3). Reproduction of CTM measurements (Figure 4a) thus requires summing up the contributions of the two molecules, each described by a spin Hamiltonian of the type:

$$\mathcal{H} = \mu_B \mathbf{B} \cdot \mathbf{g} \cdot \hat{\mathbf{S}} + \mu_B \hat{\mathbf{S}} \cdot \mathbf{A} \cdot \hat{\mathbf{I}}, \quad (3)$$

where **A** accounts for the hyperfine interaction between the copper(II) unpaired electron and nuclear spins. Satisfactory simulations were obtained with $g_{||}$ = 2.0925 and $g_{\perp}$ = 2.0227 (CTM curves are not sensitive to **A**) [36]. Figure 4b depicts CD-TDESR spectra recorded on a 1.5 × 1.0 × 0.3 mm^3 single crystal of Cu-mnt at different fields and angles. For each field/angle combination, a single clear resonance line is observed. The peak positions are well reproduced on the basis of Equation (3) with the same g-values given above (Figure 4b). The shift of the resonance line due to the angle dependence of the effective g value is barely resolved within the experimental resolution. In addition, the hyperfine coupling is not resolved. The field-dependence of the resonance line intensity is due to the frequency dependence of the source intensity.

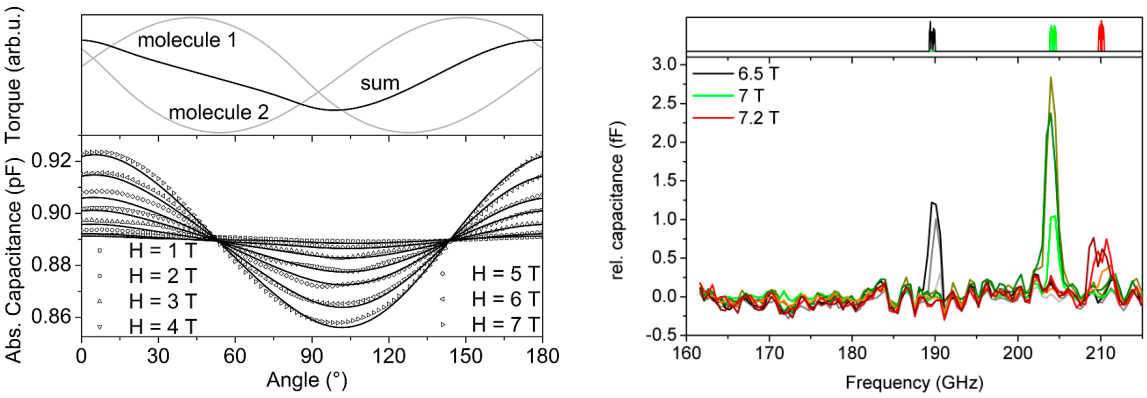

Figure 4. (**a**) capacitance as a function of angle for a single crystal of Cu-mnt at 7 K and different fields as indicated. The upper panel displays the individual contributions of the two molecules in the monoclinic unit cell; (**b**) capacitively detected frequency-domain TDESR spectra recorded on a single crystal of Cu-mnt at 2 K at different fields as indicated. Spectra are reported for different angles arising from different angles θ = 20° (light grey, light green, orange), 30° (grey, green, red), and 40° (dark grey, olive, dark red). The upper graph shows the simulated electron spin resonance (ESR) absorption spectra with parameters given in the text.

3. Discussion

In the previous sections, we have demonstrated that essentially any type of magnetic anisotropy is sufficient to generate a finite magnetic torque signal, allowing the successful recording of TDESR spectra. This greatly enhances the applicability of this emerging technique. Optically detected measurements employing a position-sensitive detector did not strongly improve sensitivity. In its current state, TDESR is not in a position to replace competing techniques, such as high-frequency ESR, as the prime experimental method to determine magnetic anisotropies. We believe that this will remain so for bulk samples. We envision that OD-TDESR may play a substantial role in investigating the properties of oriented thin layers of magnetic materials, especially when implementing interferometric detection of the reflected laser beam inside the cryostat, thus eliminating the influence of relative vibrations of the detector with respect to the cryostat.

4. Materials and Methods

TDESR spectra were recorded by using a previously described home-built spectrometer [20]. Fe_4 [37], Mn_{12} [38], V_{15} [39], and Cu-mnt [36] were prepared as previously published.

Supplementary Materials: The following are available online at www.mdpi.com/2312-7481/2/2/25/s1, Figure S1: (**a**) Starting orientation for the cantilever torque magnetometry (CTM) measurement, indicating the crystal [0 0 1] (*c*-)axis and the direction of the external magnetic field B_0; (**b**) Angle dependent CTM measurements recorded on a single crystal of Mn_{12} at 8 K and different fields as indicated. Figure S2: (**a**) Schematic picture of the spin structure of V_{15}; (**b**) Starting orientation for the CTM measurement, indicating the crystal (1 1 1) plane and the direction of the external magnetic field B_0; (**c**) Qualitative energy level diagram of V_{15} as a function of field. Figure S3: Starting orientation for the CTM measurement on Cu-mnt, indicating the crystal *b*-axis and the direction of the external magnetic field B_0.

Acknowledgments: We thank Deutsche Forschungsgemeinschaft DFG (DR228/43-1, TRR21), Fonds der Chemischen Industrie and the Deutscher Akademischer Austauschdienst//Ministry of Education, Youth and Sports (DAAD/MEYS) grant 57154055 for funding. We thank Wolfgang Frey (Institut für Organische Chemie, Universität Stuttgart) for help with indexing the crystals.

Author Contributions: Joris van Slageren, Lapo Bogani and Martin Dressel conceived the research, María Dörfel and Joris van Slageren designed the experiments, María Dörfel, Michal Kern, and Heiko Bamberger carried out all experimental work. María Dörfel analyzed all data, Joris van Slageren and Petr Neugebauer supervised all experimental work, Katharina Bader, Raphael Marx, Andrea Cornia, Tamoghna Mitra and Achim Müller synthesized the samples, and María Dörfel and Joris van Slageren wrote the paper.

Conflicts of Interest: The authors declare no conflict of interest.

Abbreviations

The following abbreviations are used in this manuscript:

CTM	Cantilever Torque Magnetometry
TDESR	Torque-Detected Electron Spin Resonance
CD	Capacitively Detected
OD	Optically Detected
HFESR	High-Frequency Electron Spin Resonance
MNM	Molecular NanoMagnet
SQUID	Superconducting Quantum Interference Device

References

1. Gatteschi, D.; Sessoli, R.; Villain, J. *Molecular Nanomagnets*; Oxford University Press: Oxford, UK, 2006.
2. Gatteschi, D.; Sessoli, R. Quantum tunneling of magnetization and related phenomena in molecular materials. *Angew. Chem. Int. Ed.* **2003**, *42*, 268–297. [CrossRef] [PubMed]
3. Woodruff, D.N.; Winpenny, R.E.P.; Layfield, R.A. Lanthanide single-molecule magnets. *Chem. Rev.* **2013**, *113*, 5110–5148. [CrossRef] [PubMed]
4. Aromí, G.; Aguila, D.; Gamez, P.; Luis, F.; Roubeau, O. Design of magnetic coordination complexes for quantum computing. *Chem. Soc. Rev.* **2012**, *41*, 537–546. [CrossRef] [PubMed]
5. Liu, J.-L.; Chen, Y.-C.; Guo, F.-S.; Tong, M.-L. Recent advances in the design of magnetic molecules for use as cryogenic magnetic coolants. *Coord. Chem. Rev.* **2014**, *281*, 26–49. [CrossRef]
6. Boulon, M.E.; Cucinotta, G.; Luzon, J.; Degl'Innocenti, C.; Perfetti, M.; Bernot, K.; Calvez, G.; Caneschi, A.; Sessoli, R. Magnetic anisotropy and spin-parity effect along the series of lanthanide complexes with DOTA. *Angew. Chem. Int. Ed.* **2013**, *52*, 350–354. [CrossRef] [PubMed]
7. Perfetti, M.; Lucaccini, E.; Sorace, L.; Costes, J.P.; Sessoli, R. Determination of magnetic anisotropy in the Lntrensal complexes (Ln = Tb, Dy, Er) by torque magnetometry. *Inorg. Chem.* **2015**, *54*, 3090–3092. [CrossRef] [PubMed]
8. Ray, K.; Begum, A.; Weyhermüller, T.; Piligkos, S.; van Slageren, J.; Neese, F.; Wieghardt, K. The electronic structure of the isoelectronic, square-planar complexes $[Fe^{II}(L)_2]^{2-}$ and $[Co^{III}(LBu)_2]^{-}$ (L^{2-} and $(LBu)^{2-}$ = benzene-1,2-dithiolates): An experimental and density functional theoretical study. *J. Am. Chem. Soc.* **2005**, *127*, 4403–4415. [CrossRef] [PubMed]
9. Haas, S.; Heintze, E.; Zapf, S.; Gorshunov, B.; Dressel, M.; Bogani, L. Direct observation of the discrete energy spectrum of two lanthanide-based single-chain magnets by far-infrared spectroscopy. *Phys. Rev. B* **2014**, *89*. [CrossRef]
10. Furrer, A.; Waldmann, O. Magnetic cluster excitations. *Rev. Mod. Phys.* **2013**, *85*, 367–420. [CrossRef]

11. Kofu, M.; Yamamuro, O.; Kajiwara, T.; Yoshimura, Y.; Nakano, M.; Nakajima, K.; Ohira-Kawamura, S.; Kikuchi, T.; Inamura, Y. Hyperfine structure of magnetic excitations in a Tb-based single-molecule magnet studied by high-resolution neutron spectroscopy. *Phys. Rev. B* **2013**, *88*. [CrossRef]
12. Boča, R. Zero-field splitting in metal complexes. *Coord. Chem. Rev.* **2004**, *248*, 757–815. [CrossRef]
13. Stoll, S. High-field EPR of bioorganic radicals. In *Electron Paramagnetic Resonance: Volume 22*; The Royal Society of Chemistry: Cambridge, UK, 2011; pp. 107–154.
14. Gatteschi, D.; Barra, A.; Caneschi, A.; Cornia, A.; Sessoli, R.; Sorace, L. EPR of molecular nanomagnets. *Coord. Chem. Rev.* **2006**, *250*, 1514–1529. [CrossRef]
15. Schweinfurth, D.; Rechkemmer, Y.; Hohloch, S.; Deibel, N.; Peremykin, I.; Fiedler, J.; Marx, R.; Neugebauer, P.; van Slageren, J.; Sarkar, B. Redox-induced spin-state switching and mixed valency in quinonoid-bridged dicobalt complexes. *Chem. Eur. J.* **2014**, *20*, 3475–3486. [CrossRef] [PubMed]
16. Van Slageren, J.; Vongtragool, S.; Gorshunov, B.; Mukhin, A.A.; Karl, N.; Krzystek, J.; Telser, J.; Müller, A.; Sangregorio, C.; Gatteschi, D.; *et al.* Frequency-domain magnetic resonance spectroscopy of molecular magnetic materials. *Phys. Chem. Chem. Phys.* **2003**, *5*, 3837–3843. [CrossRef]
17. Cornia, A.; Mannini, M. Single-molecule magnets on surfaces. In *Molecular Nanomagnets and Related Phenomena*; Gao, S., Ed.; Springer: Berlin/Heidelberg, Germany, 2015; pp. 293–330.
18. Bogani, L.; Wernsdorfer, W. Molecular spintronics using single-molecule magnets. *Nature Mater.* **2008**, *7*, 179–186. [CrossRef] [PubMed]
19. Van Slageren, J. New directions in electron paramagnetic resonance spectroscopy on molecular nanomagnets. *Top. Curr. Chem.* **2012**, *321*, 199–234. [PubMed]
20. El Hallak, F.; van Slageren, J.; Dressel, M. Torque detected broad band electron spin resonance. *Rev. Sci. Instrum.* **2010**, *81*. [CrossRef] [PubMed]
21. El Hallak, F.; Neugebauer, P.; Barra, A.L.; van Slageren, J.; Dressel, M.; Cornia, A. Torque-detected ESR of a tetrairon(III) single molecule magnet. *J. Magn. Reson.* **2012**, *223*, 55–60. [CrossRef] [PubMed]
22. Takahashi, H.; Ohmichi, E.; Ohta, H. Mechanical detection of electron spin resonance beyond 1 THz. *Appl. Phys. Lett.* **2015**, *107*. [CrossRef]
23. Rugar, D.; Budakian, R.; Mamin, H.J.; Chui, B.W. Single spin detection by magnetic resonance force microscopy. *Nature* **2004**, *430*, 329–332. [CrossRef] [PubMed]
24. Cornia, A.; Gatteschi, D.; Sessoli, R. New experimental techniques for magnetic anisotropy in molecular materials. *Coord. Chem. Rev.* **2001**, *219*, 573–604. [CrossRef]
25. El Hallak, F. Magnetic Anisotropy of Molecular Nanomagnets. Ph.D. Thesis, University of Stuttgart, Stuttgart, Germany, 25 August 2009.
26. Kern, M. Optical Setup for Torque Detected Electron Spin Resonance Spectroscopy. Master's Thesis, Brno University of Technology, Brno, Czech Republic, 22 June 2015.
27. Cornia, A.; Affronte, M.; Jansen, A.G.M.; Gatteschi, D.; Caneschi, A.; Sessoli, R. Magnetic anisotropy of Mn-12-acetate nanomagnets from high-field torque magnetometry. *Chem. Phys. Lett.* **2000**, *322*, 477–482. [CrossRef]
28. Dörfel, M. Single Crystal Studies of the Magnetic Anisotropy of Molecular Nanomagnets. Ph.D. Thesis, University of Stuttgart, Stuttgart, Germany, 29 January 2016.
29. Barra, A.L.; Gatteschi, D.; Sessoli, R. High-frequency EPR spectra of a molecular nanomagnet: Understanding quantum tunneling of the magnetization. *Phys. Rev. B* **1997**, *56*, 8192–8198. [CrossRef]
30. Tarantul, A.; Tsukerblat, B. The nanoscopic V_{15} cluster: A unique magnetic polyoxometalate. In *Molecular Cluster Magnets*; Winpenny, R., Ed.; World Scientific Publishing: Singapore, 2011; pp. 109–179.
31. Chaboussant, G.; Ochsenbein, S.T.; Sieber, A.; Gudel, H.U.; Mutka, H.; Muller, A.; Barbara, B. Mechanism of ground-state selection in the frustrated molecular spin cluster V_{15}. *Europhys. Lett.* **2004**, *66*, 423–429. [CrossRef]
32. Chiorescu, I.; Wernsdorfer, W.; Müller, A.; Miyashita, S.; Barbara, B. Adiabatic Landau-Zener-Stuckelberg transition with or without dissipation in the low-spin molecular system V_{15}. *Phys. Rev. B* **2003**, *67*. [CrossRef]
33. Tsukerblat, B.; Tarantul, A.; Müller, A. Low temperature EPR spectra of the mesoscopic cluster V_{15}: The role of antisymmetric exchange. *J. Chem. Phys.* **2006**, *125*. [CrossRef] [PubMed]
34. Gysler, M.; Schlegel, C.; Mitra, T.; Müller, A.; Krebs, B.; van Slageren, J. Spin-forbidden transitions in the molecular nanomagnet V_{15}. *Phys. Rev. B* **2014**, *90*. [CrossRef]

35. Vongtragool, S.; Gorshunov, B.; Mukhin, A.A.; van Slageren, J.; Dressel, M.; Müller, A. High-frequency magnetic spectroscopy on the molecular magnetic cluster V_{15}. *Phys. Chem. Chem. Phys.* **2003**, *5*, 2778–2782. [CrossRef]
36. Bader, K.; Dengler, D.; Lenz, S.; Endeward, B.; Jiang, S.-D.; Neugebauer, P.; van Slageren, J. Room temperature quantum coherence in a potential molecular qubit. *Nat. Commun.* **2014**, *5*. [CrossRef] [PubMed]
37. Gregoli, L.; Danieli, C.; Barra, A.-L.; Neugebauer, P.; Pellegrino, G.; Poneti, G.; Sessoli, R.; Cornia, A. Magnetostructural correlations in tetrairon(III) single-molecule magnets. *Chem. Eur. J.* **2009**, *15*, 6456–6467. [CrossRef] [PubMed]
38. Eppley, H.J.; Christou, G. Synthesis of dodecaoxohexadecacarboxylatotetraaquo-dodecamanganese $[Mn_{12}O_{12}(O_2CR)_{16}(H_2O)_4]$ (R = Me, Et, Ph, CR) complexes. *Inorg. Synth.* **2002**, *33*, 61–66.
39. Müller, A.; Döring, J. A novel heterocluster with D_3-symmetry containing twenty-one core atoms: $[As_6V_{15}O_{42}(H_2O)]^{6-}$. *Angew. Chem. Int. Ed. Engl.* **1988**, *27*. [CrossRef]